ELSEVIER

15 February 1998

OPTICS COMMUNICATIONS

Optics Communications 147 (1998) 333–340

Full length article

Temporal pulse response of a Cantor filter

F. Garzia, P. Masciulli, C. Sibilia, M. Bertolotti

Dipartimento di Energetica, Università degli Studi di Roma 'La Sapienza', and GNEQ of CNR and INFM, Via A. Scarpa 14, 00161 Rome, Italy

Received 31 July 1997; revised 4 August 1997; accepted 9 September 1997

Abstract

The response of a Cantor Fabry-Perot to a Gaussian pulse is theoretically investigated by using the transfer function of the device. A compression of the input pulse may result, if an optimum input pulse width is chosen. © 1998 Elsevier Science B.V.

1. Introduction

Self-similar structures have been studied in many physical branches. In fact the geometrical fractal properties are reflected in physical properties. This circumstance makes fractal structures interesting both for basic physics and for applications in device development.

Recently attention has been paid to the optical transmission properties of one-dimensional dielectric integrated resonators realized by a refractive index distribution that follows the Fibonacci [1,2] or the triadic Cantor [3–5] sequence. The fractal properties of the structure lead to a transmission spectrum that exhibits isolated peaks in the middle of the frequency gaps [3] and it is possible to have a field localization for the mode pattern [4]. This transmission spectrum could be used with advantages in nonlinear devices [5].

In the present paper we discuss the temporal pulse response of a Cantor filter, realized through a layered disposition of dielectric materials with suitable refractive indices, as described in Ref. [3]. We assume that a TE pulse travels through the filter.

In Section 2 we describe briefly the filtering spectral properties of the structure, in Section 3 we present the temporal pulse response and in Section 4 some results and the discussions are given.

2. Cantor filter

For the sake of clarity we first introduce very briefly the self-similarity and Cantor set concepts. An object is said to be self-similar when it is invariant with respect to a change of scale, by a fixed factor. It is possible to obtain a self-similar structure by repeating a given operation on ever smaller scales. The operation is defined over an object called *initiator*. The result of the operation applied to the initiator, is the *generator*. The self-similarity is a fractal property. The triadic Cantor set is an example of a self-similar object and is generated as follows. Take a real line (initiator) between 0 and 1 including the two end points and wipe out the open middle third, that is the interval $(1/3, 2/3)$. The intervals $(0, 1/3)$ and $(2/3, 1)$ represent the generator. Next erase the open middle third of each remaining third, and so forth ad infinitum. This procedure gives rise to an uncountable set of points, i.e. it does not exist a single connected line segment. This set, the triadic Cantor set, is a self-similar structure with a scale factor of 3. In Fig. 1a the first three levels of the Cantor set generation are shown [3].

Consider now two non-dispersive planar dielectric layers of refractive index n_2 and n_1 ($n_2 > n_1$) respectively of thickness such that their optical path is the same. Let us consider the layer of refractive index n_2 as the initiator. If L is the optical thickness of the initiator, the generator is

PII S0030-4018(97)00523-3

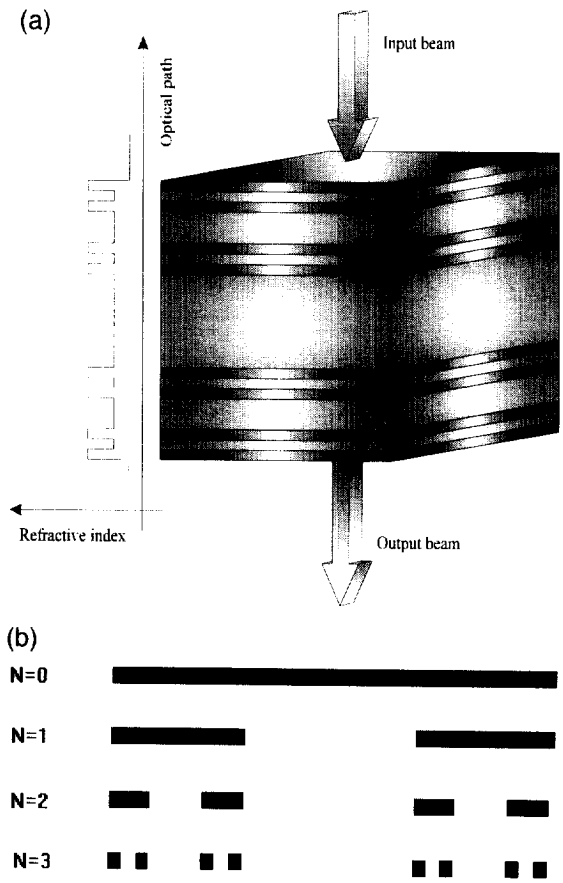

Fig. 1. (a) $N = 0$ is the initiator of the Cantor sequence, $N = 1$ is the generator. The dark regions correspond to the layers with $n_2 = 3$, while the white regions correspond to the layers with $n_1 = 1.524$. The refractive index of the two embedding layers is $n = 1.515$. (b) Refractive index distribution and resonator configuration for the level $N = 3$.

obtained by substituting the central part of the initiator, having an optical thickness of $L/3$, with a layer of refractive index n_1 and optical thickness $L/3$. The filter is obtained by iterating the operation up and down, and stopping it at the Nth step (see Fig. 1b). We consider the filter embedded between two equal semi-infinite non-dispersive layers of refractive index n less than both n_2 and n_1. The incident light is assumed to be a plane wave propagating in the direction having an angle θ with respect to the normal at the interfaces' planes.

We use the transfer matrix method [6], in order to evaluate the transmission spectrum. We consider a linear polarization of the electric field, parallel to the interface planes of the filter. Stopping the generation of the Cantor sequence at the level N, the filter is made by $2^{N+1} - 1$ stacked layers and therefore the number of interfaces is 2^{N+1}. The electric field (V) and its derivative (I) with respect to the x direction (Fig. 1b) at the substrate-last layer interface, are linked to the ones at the cladding-first layer interface by means of the following equation,

$$\begin{pmatrix} V_{2^{N+1}} \\ I_{2^{N+1}} \end{pmatrix} = \mathbf{T}^{(N)} \begin{pmatrix} V_1 \\ I_1 \end{pmatrix}, \tag{1}$$

where the transfer matrix $\mathbf{T}^{(N)}$ of the structure is obtained by the Nth iteration of the following recursive relation,

$$\mathbf{T}^{(k)}(L) = \mathbf{T}^{(k-1)}(L)\mathbf{T}_1(3^{k-1}L)\mathbf{T}^{(k-1)}(L), \quad k = 1,2,\ldots,N, \tag{2}$$

with

$$\mathbf{T}^{(0)}(L) = \mathbf{T}_2(L), \tag{3}$$

and

$$\mathbf{T}_h(L) = \begin{pmatrix} \cos(\varphi_h/3) & (1/k_{x_h})\sin(\varphi_h/3) \\ -k_{x_h}\sin(\varphi_h/3) & \cos(\varphi_h/3) \end{pmatrix}, \quad h = 1,2, \tag{4}$$

where $\varphi_h = k_{x_h}L/n_h$, $k_{x_h} = K_0\sqrt{n_h^2 - n_{\text{eff}}^2}$, $n_{\text{eff}} = n\sin\theta$, θ being the input incidence angle; k_0 is the vacuum wavenumber. The indices $h = 1, 2$ refer to the layers with refractive index n_1 and n_2 respectively. If a_c is the amplitude of the incident electric field from the cladding, then the transmission t of the filter is given by the ratio $V_{2^{N+1}}/a_c$, e.g.

$$t(k_0,L) = 2\left[T_{22}^{(N)}(k_0,L) - \frac{T_{21}^{(N)}(k_0,L)}{\mathrm{i}k_x} - \mathrm{i}k_x T_{12}^{(N)}(k_0,L) + T_{11}^{(N)}(k_0,L)\right]^{-1}, \tag{5}$$

where i is the imaginary unit, $T_{hk}^{(N)}$ are the elements of the $\mathbf{T}^{(N)}$ matrix and $k_x = k_0\sqrt{n_h^2 - n_{\text{eff}}^2}$.

In the case of normal incidence ($\theta = 0$) $\varphi_1 = \varphi_2 = \varphi = k_0 L$ it is possible to show that the magnitude of the transmission is a symmetric function of the frequency, for a fixed optical path L of the generator, and it is periodic with period $\varphi_p = 3\pi$; note that, in this case, the k_0 parameter appears only in the off diagonal elements of the $\mathbf{T}^{(N)}$ matrix, as follows from Eq. (4). In Eq. (4), the transmission depends on the φ variable alone. Moreover the diagonal and off diagonal elements of the matrices are symmetric and antisymmetric functions, respectively. This means that the real part of the transmission is a symmetric function, while its imaginary part is an antisymmetric function, of the φ variable, respectively. In other words the magnitude of the transmission is a symmetric function of the φ variable. The transmission is a periodic function of the frequency because the smallest components resonate when

$$\varphi/3 = m\pi, \tag{6}$$

with m an integer.

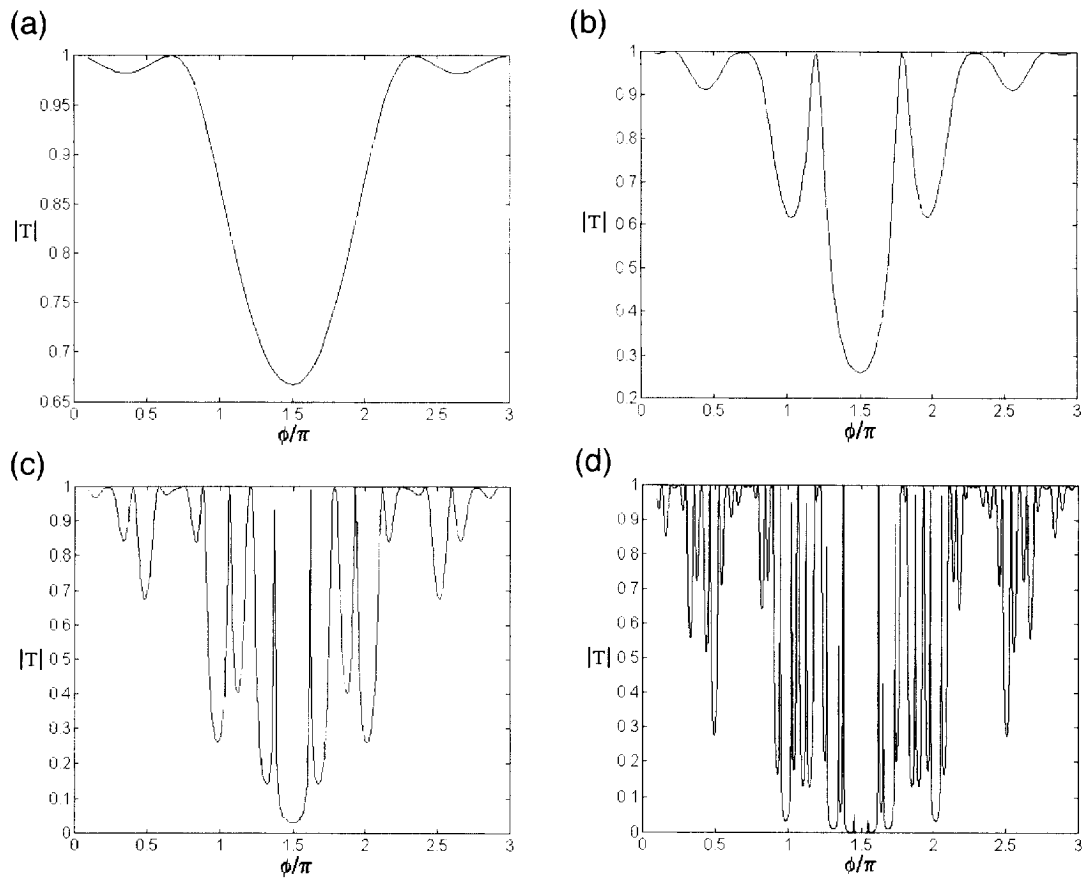

Fig. 2. Transmission $|t|$ versus φ/π for the first four Cantor levels.

An example of the transmission spectra for normal incidence is given in Fig. 2; the magnitude of the transmission as a function of φ, for the four first levels of the Cantor sequence, is shown. The considered range of φ corresponds to one period of the transmission. We note that by increasing the number N, the holes present in the spectrum become deeper. Already for $N = 3$ they merge so to give a forbidden gap of frequencies for which the transmission is zero with some isolated peaks inside (Figs. 2c, 2d).

3. Temporal response of the filter

In the previous section the Cantor filter transmission spectrum has been written as a function of the vacuum wave number $k_0 = \omega/c$ with ω the pulsation and c the vacuum light speed. The incident and the transmitted beam can be seen as the Fourier transform of a time dependent input signal $x(t)$ and a time dependent output signal $y(t)$ respectively. In what follows the signals' Fourier transform will be represented by capital letters, while the lower case letters will be used to represent signals in time domain. The transmission represents the transfer function of a linear filter:

$$H(\omega) = 2\left[T_{22}^{(N)}(\omega) - \frac{c}{i\omega n}T_{21}^{(N)}(\omega) - \frac{i\omega n}{c}T_{12}^{(N)}(\omega) + T_{11}^{(N)}(\omega)\right]^{-1}, \tag{7}$$

so that the output (transmitted) signal is given by the following equation:

$$Y(\omega) = H(\omega)X(\omega), \tag{8}$$

which can be expressed in the time domain as follows:

$$y(t) = h(t) * x(t), \tag{9}$$

where the operator $*$ means convolution integral between functions.

The function $h(t)$ is the filter impulsive response and corresponds to the inverse Fourier transform of the transfer function (7).

The input signal is an amplitude modulation of the carrier at the optical frequency ω_0:

$$x(t) = x_m(t)\cos(\omega_0 t + \theta), \tag{10}$$

in which $x_m(t)$ represents the pulse shape (envelope) and

θ is a constant temporal phase shift. Remembering that the input signal can be expressed in terms of the analytical signal $x^+(t) = (1/2\pi)\int_0^{+\infty} X(\omega)e^{-i\omega t}\,d\omega$:

$$x(t) = 2\,\mathrm{Re}\{x^+(t)\}, \tag{11}$$

or in terms of the complex envelope $\underline{x(t)} = x_m(t)e^{-i\theta}$:

$$x(t) = \mathrm{Re}\left[\underline{x(t)}e^{-i\omega_0 t}\right], \tag{12}$$

from Eqs. (9) and (10), we have

$$\underline{x(t)} = 2x^+(t)e^{i\omega_0 t}, \tag{13}$$

which in frequency domain, becomes

$$\underline{X(\omega)} = 2X^+(\omega + \omega_0). \tag{14}$$

Eq. (14) can be applied to any signal, even to the impulsive response $h(t)$. So that, with the help of Eq. (9), we have

$$\underline{Y(\omega)} = \tfrac{1}{2}\underline{H(\omega)} \cdot \underline{X(\omega)}. \tag{15}$$

This means that also the output (transmitted) signal is an amplitude modulation of the carrier at the optical frequency ω_0:

$$y(t) = \mathrm{Re}\left[\underline{y(t)}e^{-i\omega_0 t}\right], \tag{16}$$

in which the Fourier transform of the complex envelope is given by Eq. (15).

We will show here that the peculiar form of the Cantor filter allows us to obtain significant pulse compression. Let us consider a Gaussian input pulse shape:

$$x_m(t) = Ae^{-(t/\tau)^2}, \tag{17}$$

and a constant phase shift $\theta = 0$ so that the input complex envelope is

$$\underline{x(t)} = Ae^{-(t/\tau)^2}, \tag{18}$$

where A is the pulse peak amplitude.

Since

$$\tau = \frac{L}{c} = \frac{1}{\omega_0}, \tag{19}$$

where c is the velocity of the wave, and using Eq. (19) we can write

$$\bar{k}_0 = k_0 L = \frac{\omega}{c}L = \omega\tau. \tag{20}$$

Using Eq. (20) we can calculate the normalized $\bar{\omega}$ as

$$\bar{\omega} = \frac{\omega}{\omega_0} = \omega\tau = \bar{k}_0, \tag{21}$$

that is the normalized frequency $\bar{\omega}$ has the same periodical form of the normalized wavevector $\bar{k}_0$.

We have already shown that the Fourier transform of a Gaussian function is still a Gaussian function characterized by a different variance with respect to the untransformed function (Eq. (22)).

It is also well known that a large temporal pulse has a narrow frequency spectrum and vice versa. This latter property is valid not only for Gaussian pulses but for all kind of pulses.

When the pulse passes through a filter, its shape remains unchanged only if the filter has a bandwidth as large as the frequency spectrum of the pulse. The narrower the bandwidth with respect to the spectrum of the pulse the larger the pulse, because the higher spectral components are stopped by the filter. If the filter is characterized by a more complex transmission function, the shape of the pulse can deeply change because of the attenuation of some spectral components, that are not necessarily the higher ones. A modulation of the original pulse can even result, if most frequencies are attenuated excepted a particular frequency or a group of frequencies centered around a narrow transmission peak.

We want now to relate the width of the Gaussian input pulse, depending on τ, to the width of the periodical structure of both $\bar{k}_0$, $\bar{\omega}$ that is equal to 3π. It is well known that the Fourier transform of the pulse expressed by Eq. (18) is

$$X(\omega) = A\tau\sqrt{\pi}\exp(-\pi^2\tau^2\omega^2), \tag{22}$$

that is still a Gaussian function whose spectral width is inversely proportional to the time width of the input pulse, as already mentioned above. This means from the theoretical point of view that, due to the infinite extension of a Gaussian function, the spectral components of the pulse extend over the typical period of $\bar{k}_0$, $\bar{\omega}$ that is 3π. In practice the mentioned function decreases to zero according to a slope that depends on τ, as can be seen from Eq. (22). If we want the transform of the pulse to be confined to the period 3π, we have to impose that the amplitude of the function expressed by Eq. (22), calculated in the extremes of the periodic interval 3π, must be less than b, where b is an arbitrary number as taken from

$$\exp\left[-\pi^2\tau^2(1.5\pi)^2\right] = b, \tag{23}$$

that can be solved with respect to τ giving:

$$\tau = \pi^2 \times 1.5^2 \log(1/b) \cong 22.21\log(1/b). \tag{24}$$

In this way it is possible to calculate τ, related to the maximum extension of the input pulse with respect to its frequency, that ensures its transform to be confined into the periodic interval mentioned.

4. Results and discussion

The compression of an optical pulse has already been studied from the theoretical and experimental point of view [7–15]. Different techniques are available to perform this operation in a rather efficient way. The compressing device presented here is based on the particular behavior

of the transfer function of a Cantor filter, that shows very sharp transmission peaks inside the forbidden band. This device is not comparable with the traditional optical fiber-based techniques in terms of energy transferred from input to output, since as we show below a consistent part of the input pulse energy is reflected, but shows interesting potential to be used as an integrated device.

We first analyze the device from the self-similar point of view and then analyze a secondary, but not less interesting, aspect that is the compression of a proper input pulse.

To observe a self-similar behavior in the temporal response of the device it is necessary to consider as much as possible the whole width of its transmission spectrum. That is, it is necessary to consider only pulses whose spectral width is as large as the one of the device, i.e. only short temporal pulses. The optimum pulse length can be rapidly obtained using the criterion expressed by Eq. (24). Fig. 4a shows the short input pulse whose spectrum is shown in Fig. 4b, where it is possible to see that it extends all over the interval considered. The following figures show the spectral behavior and the temporal behavior respectively for different values of N. The temporal extension of the interval for lower values of N has been properly magnified to better analyze the self-similar properties. It is immediate to see that the pulse spread out over a large temporal interval due to the fact that the higher the order N, the more discontinuous the spectral transmission of the device becomes, adding and subtracting new frequencies that modulate the output pulse. Further it is possible to see that the higher the order, the lower the central peak of the device, because of the constant energy of the pulse. This means that if the pulse is distributed over a longer interval, the central peak must unavoidably decrease. It is anyway possible to see that the output pulse shows a self-similar behavior, that reflects the self-similar behavior of the transmission spectrum of the device. We now consider the other interesting behavior of the device, that is the compression effect that takes place when the spectrum of the pulse is narrower than the spectrum of the device.

We have already shown that a Cantor filter is characterized by a certain number of transmission peaks inside the forbidden band, whose number and sharpness increase with the order N of the Cantor generation code.

To be specific in our numerical calculations we consider a structure made of materials with the following refractive indexes: $n_{01} = 1.35$, $n_{02} = 2.3$, at a wavelength $\lambda_0 = 1.06$ μm.

The cases of $N = 1,2$ are not very interesting since the properties of the self-similar filter are not very evident. We consider the situation $N \geq 3$. In particular we restrict our analysis to $N = 3$, since the other situations are perfectly analogous. For the considered materials the transmission function for $N = 3$ is shown in Fig. 3a. It is possible to see that two sharp peaks are present in the forbidden band indicated in the figure by two arrows. We will compare the

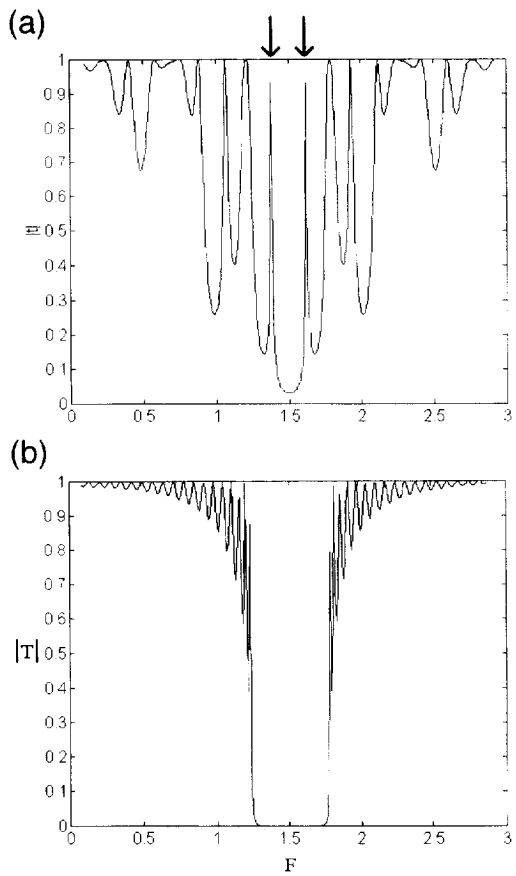

Fig. 3. (a) Transmission spectrum of a Cantor Fabry-Perot for $N = 3$. (b) The same as (a) but for a periodic structure.

obtained results with the behavior of a periodic filter whose forbidden band is as large as the one of the Cantor device, without considering the first transmission peaks. The transmission function of the periodic filter is shown in Fig. 3b; this periodic filter has the same optical path as the Cantor one. In this way it is possible to compare the response of both structures when a pulse, whose frequency spectrum varies from the situation of total confinement inside the forbidden band to the situation of extension over the forbidden band, passes through the devices.

If the input pulse has the form expressed by Eq. (10) three different situations can arise. The first one is the most trivial and appears when the Fourier transform of the pulse lies between the two peaks indicated by the arrows in Fig. 3a (wide pulse): in this case the spectral components of the pulse are filtered by the flat and near to zero zone of the transmission function, and therefore the pulse emerges from the device unaltered from the compression point of view but strongly attenuated. The same occurs if the pulse passes through the periodic structure.

The second situation arises when the Fourier transform of the pulse extends to cover the two peaks of the filter

(optimal pulse): in this case all the spectral components are attenuated and rejected towards the input excepted the components relative to the two transmission peaks. Modulation of the original pulse according to the frequency relative to the two peaks occurs, and the output pulse is composed by a train of narrow pulses, where the total temporal extension is longer than the length of the original pulse, but the temporal extension of the single pulse is

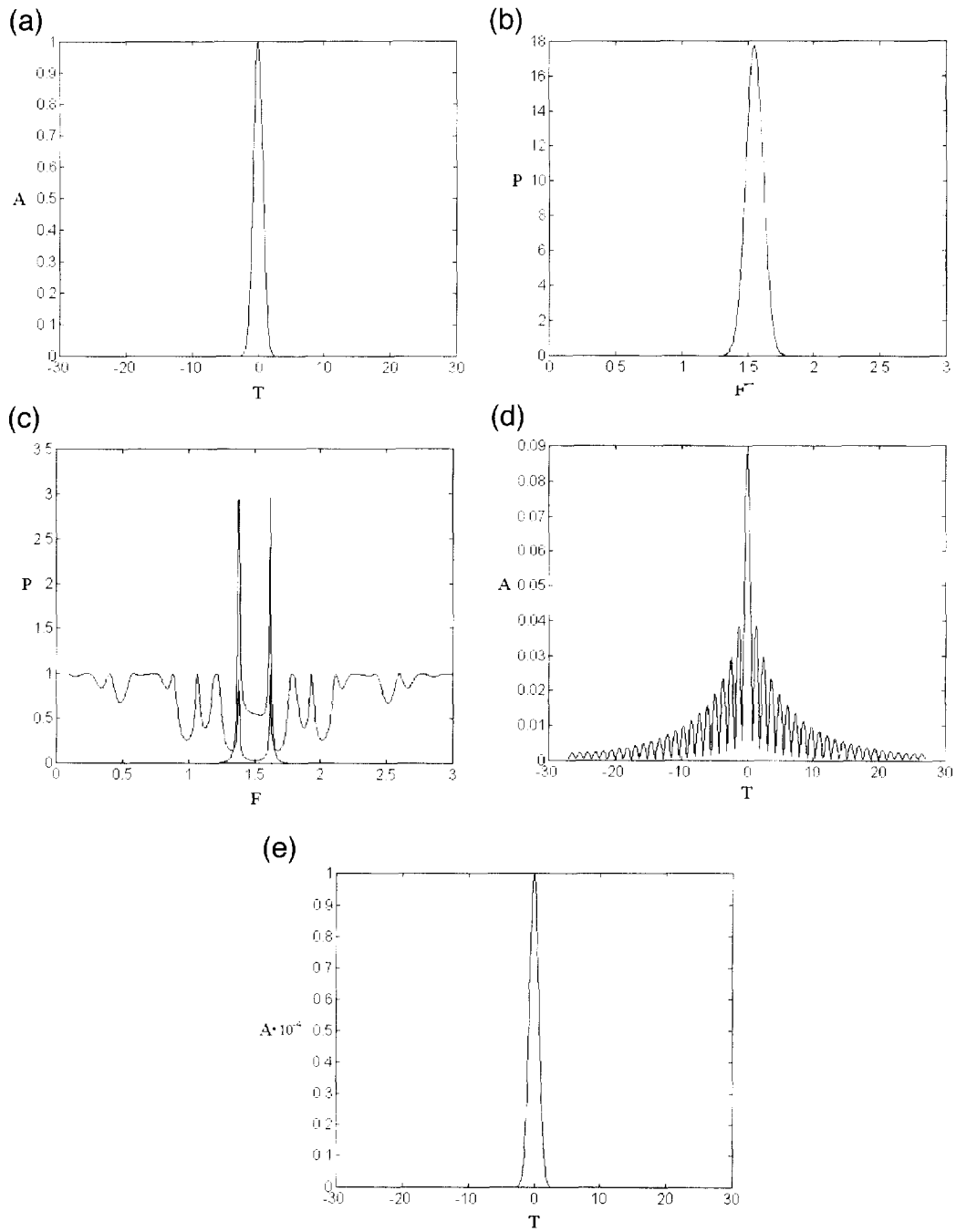

Fig. 4. (a) Input pulse for $1/\tau = 1$. T is the time normalized to $1/\omega_0$. A is the amplitude. (b) Frequency spectrum of the input pulse for $1/\tau = 1$. F is the frequency normalized to $k_0 L/\pi$. (c) Transmission spectrum of the Cantor filter superimposed to the frequency spectrum of the output pulse. The input pulse is characterized by $1/\tau = 1$. (d) Output pulse from the Cantor filter. The input pulse is characterized by $1/\tau = 1$. (e) Output pulse from the periodic filter. The input pulse is characterized by $1/\tau = 1$.

shorter than the length of the original pulse. The train of output pulses is characterized anyway by a central intense pulse whose amplitude is almost twice the amplitude of the first lateral pulses, and therefore easily detectable. After a proper filtering action to eliminate the undesired output components, a compression of the input pulse occurs, even if part of the energy has been reflected back to the input. This is shown in Fig. 4. If the pulse passes through a traditional structure, the result is analogous to the previous results.

The third situation arises when the Fourier transform of the pulse extends well over the two peaks (narrow pulse): in this case the spectral components of the pulse show a larger irregular zone of the transmission function, and therefore the pulse emerges from the device altered, but not very attenuated since most of its spectral energy is able to pass through the device. In this case the behavior strictly depends on the peaks of the spectral components of the input pulse and on their relative modulation action. A complex compressing behavior arises, anyway not very efficient as the previous one, but with a reasonably good input–output energy ratio. If the pulse passes through a periodic structure, the result is analogous to the result obtained for the Cantor structure, even if the peaks of the transmission spectrum are more regular.

The results obtained until this point show that the Cantor structure shows a peculiar compressing behavior that is not present in a more traditional periodic structure.

To evaluate the compressing capacity of the Cantor device with respect to the length of the pulse it is necessary to introduce some parameters. The first parameter is the compression ratio (CR), that is the ratio between the width at half height of the input pulse and the width at half height of the output pulse. If compressing behavior is present, the output pulse is obviously narrower than the input pulse and CR is greater than one. In Fig. 5, CR as a function of the input pulse value $1/\tau$ is shown for our Cantor filter. It is possible to see that CR is maximum when $1/\tau$ is equal to 1. The irregular behavior of the curve is due to the fact that when the input pulse becomes narrower, its transform becomes wider and presents different peaks of the transmission spectrum of the device. This behavior gives place to sudden transmission of the pulse.

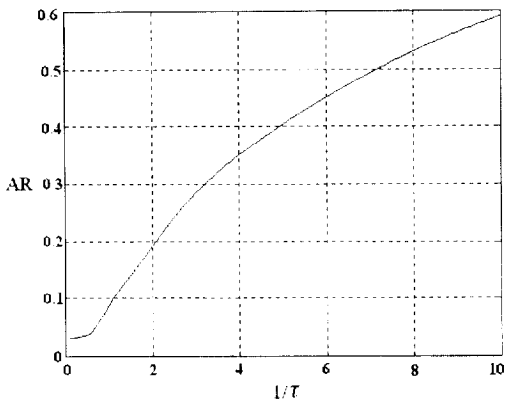

Fig. 6. Amplitude ratio (AR) as a function of $1/\tau$.

The second parameter is the amplitude ratio (AR), that is the ratio between the amplitude of the output pulse and the amplitude of the input pulse. It is generally less than one because of unavoidable attenuation always present. It gives an idea of the amount of energy transferred from the input to the output. In Fig. 6 the AR as a function of $1/\tau$ of the input pulse is shown. It is possible to see that AR increases with $1/\tau$. This is due to the fact that the narrower the input pulse, the wider its transform, so that there are zones of the transmission spectrum where it is not attenuated.

The third parameter that summarizes the first two are the compression efficiency (CE) that is given by the product of the compression ratio by the amplitude ratio. It is shown in Fig. 7. It is possible to see that it increases with $1/\tau$, because of the increasing behavior of AR. If we are mainly interested on the compressing behavior of the device we have mainly to focus our attention on CR, that reaches its maximum when $1/\tau = 1$. If we are interested

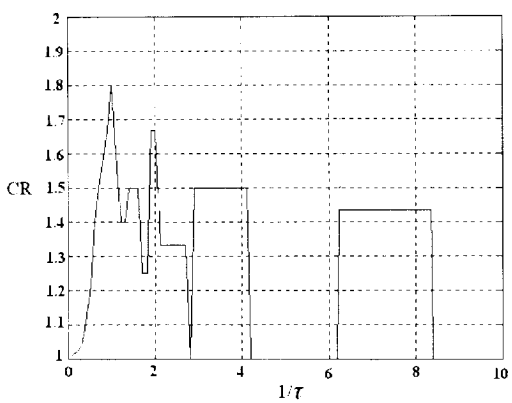

Fig. 5. Compression ratio (CR) as a function of $1/\tau$.

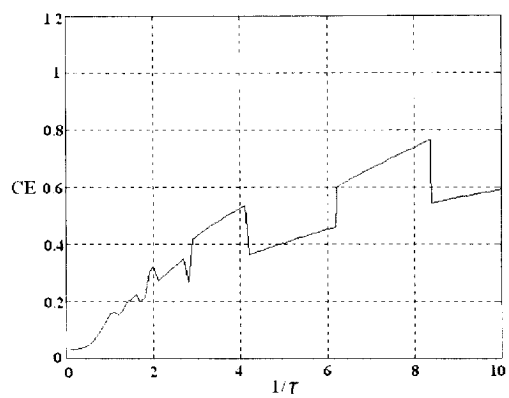

Fig. 7. Compression efficiency as a function of $1/\tau$.

both on compression and on energy transfer we have to focus our attention on CE that reaches its maximum when $1/\tau$ is equal to about 8.2.

All the above considerations are valid only if the materials used for the devices are linear. In fact this allows us to consider the output pulse as a superposition of each frequency composing the input pulse. Further the behavior of the device does not depend on the input intensity.

5. Conclusions

A pulse compressor device based on the properties of a Cantor filter has been presented. It has been compared with a periodic one, showing interesting results, in fact it can be accurately designed to show its maximum compressing behavior for a desired input pulse length and wavelength.

References

[1] W. Gellerman, M. Kohmoto, B. Sutherland, P.C. Taylor, Phys. Rev. Lett. 72 (1994) 633.
[2] R. Riklund, M. Severin, J. Phys. C 21 (1988) 3217.
[3] M. Bertolotti, P. Masciulli, C. Sibilia, Optics Lett. 19 (1994) 777.
[4] M. Bertolotti, P. Masciulli, C. Sibilia, SPIE 2212 (1994) 607.
[5] M. Bertolotti, P. Masciulli, C. Sibilia, F. Wijnands, H. Hoekstra, J. Opt. Soc. Am. B 13 (1996) 628.
[6] M. Born, E. Wolf, Principles of Optics, 5th ed. Pergamon, Oxford, 1972, p. 51.
[7] W.J. Tomlinson, R.H. Stolen, C.V. Shank, J. Opt. Soc. Am. B 1 (1984) 139.
[8] D. Grischkowsky, A.C. Balant, Appl. Phys. Lett. 41 (1982) 1.
[9] I.P. Christov, IEEE J. Quantum. Electron. 24 (1988) 1548.
[10] W.N. Knox, R.L. Fork, M.C. Downer, R.H. Stolen, C.V. Shank, J.A. Valdmanis, Appl. Phys. Lett. 46 (1985) 1120.
[11] J.M. Halbout, D. Grischkowsky, Appl. Phys. Lett. 45 (1984) 1281.
[12] R. Thurston, J. Heritage, A. Wiener, W. Thomlinson, IEEE J. Quantum Electron. QE-22 (1986) 682.
[13] C.V. Shank, R.L. Fork, R. Yen, R.H. Stolen, W.J. Tomlinson, J. Opt. Soc. Am. B 1 (1984) 139.
[14] B. Nikolaus, D. Grischkowsky, Appl. Phys. Lett. 42 (1983) 1.
[15] B. Nikolaus, D. Grischkowsky, Appl. Phys. Lett. 43 (1983) 228.